EXPERIMENTAL STUDY ON AERODYNAMIC CHARACTERISTICS OF CABLES WITH PATTERNED SURFACES

Toshio MIYATA,* Hitoshi YAMADA,** and Tetsuo HOJO***

When constructing super long span cable-stayed bridges, aerodynamic cable sections with suppressing vibration and a low drag coefficient are required. With emphasis on the surface roughness of cables, experiments have been carried out to reduce drag coefficients and control rain-induced vibrations. These experiments verified that, over the range of design wind velocities (or a Reynolds number of about 5.5×10^5), cables given a relative surface roughness of about 1% of the cable diameter have approximately the same drag coefficient as cables with a smooth surface. Through measurements of the pressure distribution around model cable, it was also ascertained that discretely surface patterned cables had the effect of raising the apparent Reynolds number and moving the separation point backward.

Key Words: cable, surface roughness, drag coefficient, rain vibration

1. INTRODUCTION

Single-strand cables protected by anti-corrosion coverings (of polyethylene for instance) have recently been widely used in the construction of long cable-stayed bridges. Vibrations induced by the combined effects of rain and wind, which are referred to as rain vibrations, have often been reported in smooth cables of this type.[1),2),3)] Extensive research into the mechanism of rain vibrations and measures to control the vibrations has been carried out, and the effects of such suppressing measures have been observed in actual bridges.[4),5),6)]

Two main techniques have been used to control rain vibrations; one is to install some kind of vibration-damping devices on the cables near the cable anchor points,[4),7)] or tie cables to distribute the vibration energy,[8)] and the other is to improve the aerodynamic characteristics of cables by introducing roughness on their surfaces.

With the recent demand for longer cables to suit the increasing span of cable-stayed bridges, there have been certain cases in which it was impossible to obtain sufficient vibration-damping effects; there is a limit to the number of places where additional vibration damping devices can be installed. Accordingly,

* Dr. Eng., Professor of Yokohama National University, Yokohama City, Kanagawa 240
** Dr. Eng., Assistant Professor of Yokohama National University, Yokohama City, Kanagawa 240
*** Senior Manager, Bridge Engineering & Construction Div., Nippon Steel Corp., Chiyoda-ku, Tokyo 100
† This is an updated translation of a paper which originally appeared in "Bridge and Foundation Engineering", Vol. 27, No. 9

aerodynamic measures are expected to become more important in the future. At the same time, since there have been cases where the design of cable-stayed bridge girders and main towers has been dictated by the wind loading on the many cables perpendicular to the bridge axis, it is necessary to look for aerodynamic cable sections with a smaller drag coefficient and better vibration-controlling characteristics.

The main objective of conventional aerodynamic cable designs has been to suppress rain vibrations by adding grooves or projections to the cable surface. However, there have been only a few studies on the overall aerodynamic performance of cables, including their drag coefficient.

Table 1 Cable Models

Model	Diameter D (m)	Surface roughness (μm)	Relative surface roughness (k/D)	Remarks
A_1	0.1315	3	2.3×10^{-5}	Smooth
A_2	0.1220	30	2.5×10^{-4}	Uniform distribution all over the surface
A_3	0.1315	100	7.6×10^{-4}	"
A_4	0.1235	200	1.6×10^{-3}	"
A_5	0.1240	600	4.8×10^{-3}	"
A_6	0.1275	1,500	1.2×10^{-2}	"
B_1	0.1465	200	1.6×10^{-3}	Grid-like pattern all over the surface
B_2	0.1465	600	4.1×10^{-3}	"
B_3	0.1490	1,200	8.1×10^{-3}	"
C_1	0.140	3	2.1×10^{-5}	Smooth
C_2	0.140	1,500	1.1×10^{-2}	Discrete concave pattern
C_3	0.140	1,500	1.1×10^{-2}	Discrete convex pattern

The drag coefficient, C_D, of a cable with a circular section increases up to 1.2 in the high Reynolds number range where the cable deforms. In this study, experimental work to reduce this drag coefficient and control rain vibration performance was carried out with particular attention to minute changes in the cable surface, or surface roughness.

Various studies have been made concerning the relationship between the surface roughness and aerodynamic properties of round cables.[12),13)] Many of these consisted of measurements and analysis of static aerodynamic properties, including the effects of surface roughness on the Reynolds number. However, studies of the effects of surface roughness on rain vibrations was hardly dealt with. There have been almost no reports of the detailed effects of shape and surface roughness distribution.

In this study, therefore, the basic aerodynamic properties of cables with approximately uniform surface roughness were first investigated using a wind tunnel. Based on the results of these experiments, more precise aerodynamic coefficients of cables with different shapes and roughness distribution patterns were then measured. To examine the rain vibration suppressing effects, wind tunnel tests were carried out with simulated rainfall, and the pressure distribution around the cable surface was measured to analyze the aerodynamic properties. Finally the surfaces of the cables used in this study were studied in detail.

2. AERODYNAMIC PROPERTIES OF CABLES WITH SURFACE ROUGHNESS

2.1 Experimental methods

To understand the effects of surface roughness on aerodynamic properties, a three-component test was carried out. Aluminum pipes with the same diameter and polyethylene coating as those used in actual bridges were used as cable models. To clarify the effects of surface roughness, models with three different shapes and surface roughness distributions were prepared.

The entire surface of Models A_1 through A_6 was roughened uniformly by attaching molten polyethylene particles through a process of thermal adhesion. The surface roughness was described in terms of an average peak-to-valley height, R_Z, taken from the roughness curve resulting from

measurements with a contact-type roughness meter. Grid-like roughness was applied over the whole surface of Models B_1 through B_3, and this roughness was described in terms of the depth of the grid. The circular concave and convex patterns was added discretely to the surface of Models C_2 and C_3, and the roughness was described in terms of the depth of the concavities or the height of the convex sections. Table 1 shows the experimental parameters for these cable models.

Experiments were implemented on Models A and B in a low-speed wind tunnel 2.0 m in section height and 1.0 m in width. This wind tunnel is at the Public Works Research Institute of the Ministry of Construction. Measurements were made up to a wind velocity of about 25 m/s, equivalent to a Reynolds number of about 2.2×10^5. Experiments on Models C were carried out in a large-scale circulating wind tunnel with a 3.0 m section height and 2.0 m width at Sumitomo Heavy Industries Co., Ltd. These measurements were extended up to almost the design wind velocity assumed for actual bridges, or about 55 m/s, where the Reynolds number is about 5.5×10^5. The ratio of wind tunnel mouth area to cross-sectional area of the model, known as the blockage ratio, was less than 7% for Models A and B and and 5% for Model C respectively. Since the geometrical ratio of the model to the end plate had a critical effect on measurements, two-dimensionality was assured by providing a sufficiently large end plate.

2.2 Experimental results

As shown in Figure 1,[14] the drag coefficient, C_D, of a circular section with smooth surface in a uniform flow is a function of the Reynolds number, $Re = VD/\nu$, where V is the flow velocity; D is the representative length; and ν is the kinematic viscosity. C_D drops sharply in the Reynolds number range about 2×10^5 to 4×10^5. In the case of typical cables used in suspension structures, say the 0.15 m-diameter cables of cable-stayed bridges, and at a wind velocity of about 50 m/s, the Reynolds number ranges approximately from 10^4 to 5×10^5. This falls into the subcritical or supercritical range.

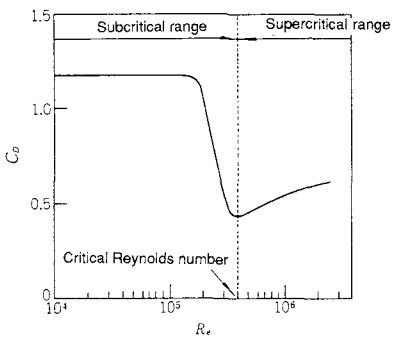

Figure 1 Relationship between the drag coefficient of a circular section and the Reynolds number

Furthermore, surface roughness causes a shift in the separation point along the body where the section is circular, and this accelerates the transition into the turbulent flow region. Since changes in drag coefficient are dominated by the location of the separation point, the surface roughness also has a great effect on the drag coefficient in the range of the critical Reynolds number.

Figures 2 through 5 show measured drag coefficients for the various models. All of these drag coefficients, C_D, are nearly equal, or about 1.2, in the subcritical range. From Figures 2 and 3, it is evident that, in the case of cables with a uniformly distributed surface roughness, the critical Reynolds number drops as the surface roughness increases. With increasing relative surface roughness, k/D, the drag coefficient at the critical Reynolds number exceeds the drag coefficient of the smooth round cable models by about 0.5. With increasing wind velocity, the drag coefficient increases and has a tendency to rapidly approach 1.2. For Model A_6, which has a uniform relative surface roughness of about 1% of its diameter, the drag coefficients are about 0.9 and 1.2 at the critical Reynolds number (about 4×10^4) and at a

Reynolds number of 2.2 x 10^5, respectively.

In this study, we also carried out experiments at smaller relative surface roughness levels than considered in previous studies. The results agreed well with those reported previously[15] within the range of relative surface roughness from 10^{-2} to $10.^{-3}$

Figure 4 shows the drag coefficients of Models B_1 through B_3, which were given approximately the same degree of surface roughness as Model A_4 through A_6 but in a grid-like pattern. The critical Reynolds number of models with this grid-like roughness decreases as the relative surface roughness increases, as with Models A_1 through A_6 having uniform surface roughness. However, the mode of increase is different from that of Models A; the drag coefficient increases gradually with increasing wind velocity. The critical Reynolds number of Model B_3, where the grid-like surface roughness is about 1% of the diameter, is about 6 x 10^4 and the drag coefficient is about 0.9 at a Reynolds number of 2.2 x 10^5.

Figure 5 shows the drag coefficients of Models C_2 and C_3, which have approximately the same degree of surface roughness as Models A_6 and B_3 but applied discretely. Experimental results of Model C_1, which has the same smooth surface as A_1, agree well with the previous study illustrated in Fig. 1. Both C_2 and C_3 have the same behavior; the critical Reynolds number and drag coefficient are 1 x 10^5 and 0.6, respectively. Within the range of measurements up to a Reynolds number of about 5.5 x 10^5, equivalent to a wind velocity of about 55 m/s, the drag coefficient remains approximately constant.

Thus, as noted in a previous study,[14] the shape and distribution of surface roughness as well as its relative size have a strong influence on drag characteristics of circular section, because they change the flow separation pattern on the surface. The experiments described above show that the models having discrete roughness have less drag force than uniform roughness in the critical range and almost same C_D value in the supercritical range up to a Reynolds number of 5.5 x 10^5. It was also proven that almost equivalent drag coefficients can be obtained with discrete roughness patterns as with smooth surfaces within the design wind velocity region. The effects of the shape and distribution pattern of surface roughness are described later.

3. EXPERIMENTS ON RAIN VIBRATION SUPPRESSING EFFECTS OF SURFACE-ROUGHENED CABLES

3.1 Experimental methods

In order to learn the rain vibration suppressing effects of surface-roughness, vibration tests under simulated rainfall were carried out. Figure 6 shows the wind tunnel apparatus used.

Models C_1 through C_3, each 3 m in length, were used for the tests. The models were freely supported on springs in the direction perpendicular to the cable axis, and fixed with piano wires in the direction of the cable axis. The model weight was 19.8 kgf, the natural frequency about 1.8 Hz, the logarithmic structural damping ratio ranged from 0.003 to 0.004, and the Scruton number ranged from 1.7 to 2.3. Table 2 shows the experimental parameters for each cable. Cable models were set up with a vertical angle, α, of 45° and a horizontal angle, β, of 45° during experiments with rainfall, and a vertical angle, α, of 45° and a horizontal angle, β, of 135° during experiments without rainfall. These experiments were done in an Eiffel type wind tunnel having a 2.5 m height and 1.5 m width and equipped with a water nozzle. To simulate water rivulet, water was supplied from a point near the higher end of the model cable.

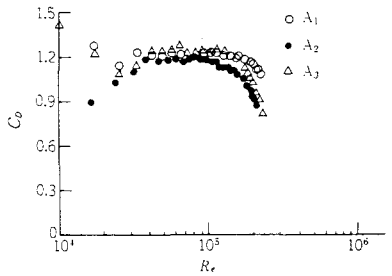

Figure 2 Relationship between the drag coefficient of Models A_1-A_3 and the Reynolds number

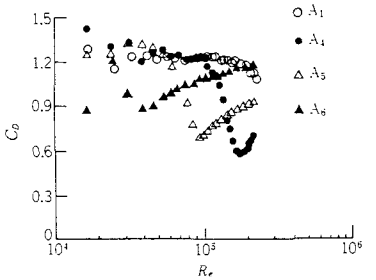

Figure 3 Relationship between the drag coefficient of Models A_4-A_6 and the Reynolds number

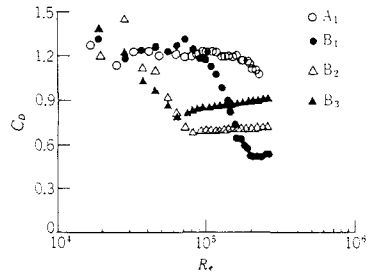

Figure 4 Relationship between the drag coefficient of Models B_1-B_3 and the Reynolds number

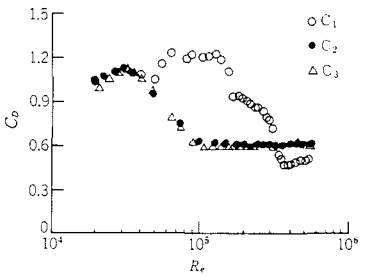

Figure 5 Relationship between the drag coefficient of Models C_1-C_3 and the Reynolds number

3.2 Results of experiments

(1) Vibration responses during rainfall

Figure 7 shows the vibration response characteristics of cable Model C_1 at water volume of 0.8, 1.4, and 2.0 lit./min. Except for a vortex-induced vibration in the low wind velocity range, vibration didn't arise during no-rainfall experiments on Model C_1 with a smooth surface. With simulated rainfall at water volume of 0.8 and 1.4 lit./min. and 2.0 lit./min., vibrations occurred at wind velocities of about 9 and 12 m/s and higher, respectively. This is a characteristic already proven by past experiments.

Figure 8 shows the damping characteristics of cables at a vibration amplitude ratio, A/D, of 0.1. Of the three water volume studied, Figure 8 makes clear that the wind velocity range within which rain vibration occurred was the widest and negative damping largest with a water volume of 0.8 lit./min.

Figure 9 shows the V-A-δ curve for Model C_1. The maximum logarithmic decrement for this cable model is about minus 0.07. In the experiment, measurements were continued up to a non-dimensional amplitude, A/D, of 1. Within this range, unstable vibrations occurred when the reduced wind velocity, V/f·D, exceeded about 40.

For Models C_2 and C_3 with roughened surfaces, on the other hand, no rain vibrations occurred, as shown in Figure 10. Thus cables with such sectional forms have vibration suppressing effects. Although Figure 10 shows only the results at a water volume of 0.8 lit./min., it was ascertained that no rain vibrations occurred in Models C_2 and C_3 at other volume under the same experimental conditions as for Model C_1.

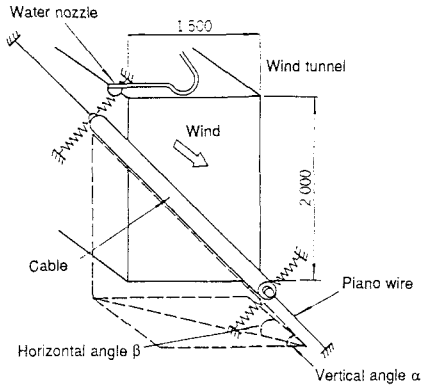

Figure 6 Rain vibration experimental apparatus

Table 2 Dimensions of Models used

Model	Weight per length (kgf/m)	Frequency (Hz)	Logarithmic decrement δ	Remarks
C_1	6.6	1.8	0.0035	Smooth
C_2	6.6	1.8	0.0039	Discrete concave pattern
C_3	6.6	1.8	0.0032	Discrete convex pattern

(2) Results of rivulet measurements

Figures 11 and 12 show the measured location and width of rivulets formed on the upper surfaces of Models C_1, C_2, and C_3 at a distance of 2.2 m from the upper end of the cable models. The location of rivulets was surveyed by reference to markings drawn around the surface of the cables. On the upper surface of Model C_1, which has a smooth surface, rivulets started forming at the same time as rain vibrations occurred, or at a wind velocity of about 9 m/s, indicating that rivulets are one of the factors leading to rain vibrations.

In the case of Models C_2 and C_3, which have patterned surfaces, the location of rivulets on the upper surface shifted downstream in comparison with Model C_1. Although the rivulets on the upper surface of Model C_1 were located at an angle θ of about 60°, the same location as noted in a previous study[11], those in the case of C_2 and C_3—where there was a vibration suppressing effect—were at 80° and 70°, respectively. The width of rivulets, $\Delta\theta$, in the case of Models C_2 and C_3 was about half that of Model C_1. These phenomena can probably be explained by the fact that surface roughness creates small concave and convex patterns on the surface, increasing the apparent Reynolds number, and moving the separation point backward. This tendency is particularly marked in Model C_2, with the greatest vibration suppressing effects, where no rivulets formed on the upper surface at wind velocities in excess of 13 m/s.

In the case of Models C_2 and C_3, which have roughened surfaces, water flowed along the concave and convex patterns in a way clearly different from the flows in Model C_1. In contrast with the stable boundaries between rivulets on the smooth surface of Model C_1, the boundaries in Models C_2 and C_3 were unstable. Thus it appears that the stable formation of rivulets can be restrained by adopting a pattern of concavities and convexities as in Models C_2 and C_3. Photos 1 and 2 show rivulets on the upper surfaces of the cable models.

(3) Vibration response without rainfall

To ascertain the vibration suppressing effects of cables with roughened surfaces, vibration tests without rainfall were conducted. The purpose of this was to ascertain the possibility of unstable cable vibrations when no rain is falling, even if no rivulets form during rainfall, as reported previously[16].

Figure 13 shows the damping characteristics of Models C_1 and C_2. For smooth-surfaced Model C_1, unstable vibrations arose at a wind velocity of about 20 m/s. With Model C_2, which has the roughened

surface, stability was seen throughout the wind velocity range, indicating that there is a suppressing effect even without rainfall.

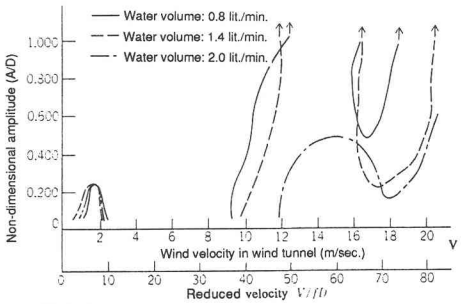

Figure 7 Vibration response characteristics

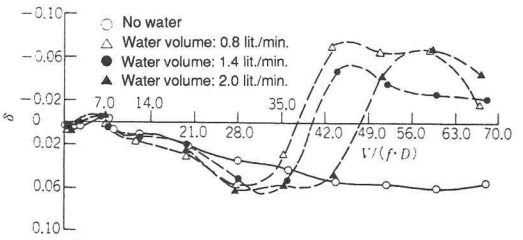

Figure 8 Damping characteristics of model C_1

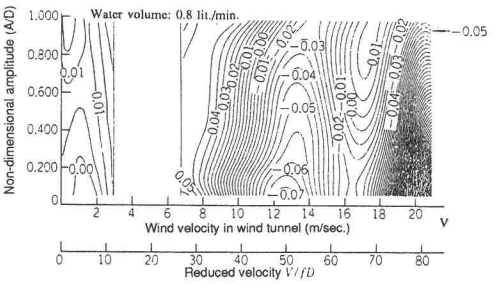

Figure 9 V-A-δ curve of Model C_1

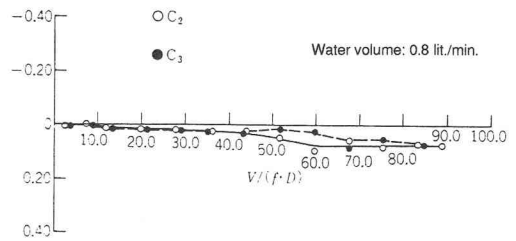

Figure 10 Damping characteristics of Models C_2 and C_3

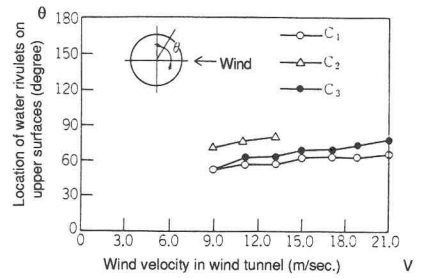

Figure 11 Location of water rivulets on upper surfaces

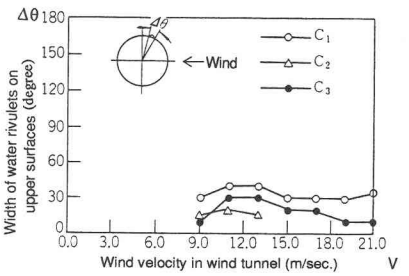

Figure 12 Width of water rivulets on upper surfaces

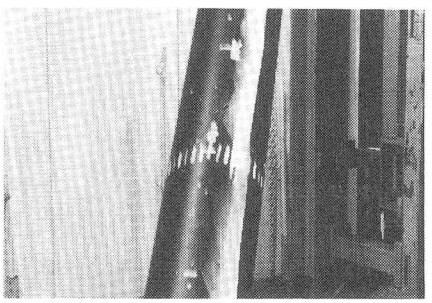

Photo 1 Water rivulets on upper surface of Model C_1

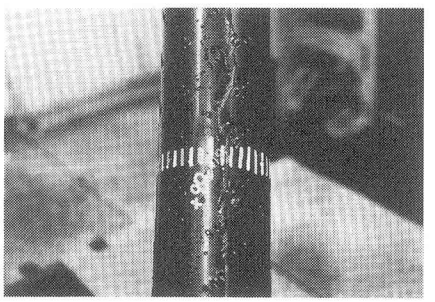

Photo 2 Water rivulets on upper surface of Model C_2

4. PRESSURE DISTRIBUTION ON CABLES WITH SURFACE ROUGHNESS

4.1 Experimental methods

Cables with a discretely roughened surface have different aerodynamic and vibration suppressing characteristics from those with smooth surfaces. Accordingly, their characteristics were analyzed in terms of pressure distribution. Cable models were set up with a vertical angle, α, of 0°, and horizontal angle, β, of 90°.

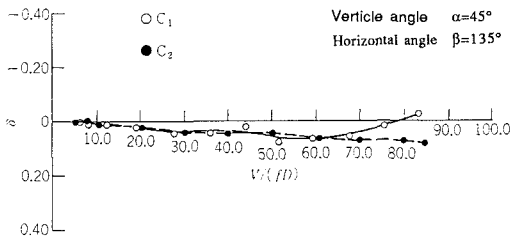

Figure 13 Damping characteristics of Models C_1 and C_2 (during no rainfall)

Measurements of the pressure distribution around cable models were made by reading pressure at 36 pressure-measuring taps embeddedin Models C_1 and C_2 circumferentially at intervals of 10°. These measurement points were connected to a pressure converter through vinyl tubes. Ultra-high-sensitivity strain gauge-type differential pressure meters were used for the measurements. The reference static pressure was measured using a Pitot tube installed in the wind tunnel itself. The non-dimensional pressure coefficient, C_P, was defined by the following equation; $Cp = (P-P_\infty)/(1/2\rho V^2)$.

4.2 Experimental results

Figure 14 shows the measured pressure coefficient for Model C_1. This shows the same characteristics as obtained in a previous experiment[17]. That is, in the subcritical range, the location of the separation point, θ, was about 80° for a Reynolds number of about 0.9 x 10^5, and the pressure coefficient on the rear surface was almost constant, showing that thorough flow separation takes place at the rear surface. The separation point θ *is defined* as transferring point where C_D curve turns from upward to level. In the supercritical range at a Reynolds number of about 5.5 x 10^5, the separation point moved backward to an angle θ of about 100°, and the static pressure on the rear surface was restored because of turbulent mixing, narrower wake width and so forth.

On the other hand, with Model C_2, no difference in pressure coefficient at Reynolds numbers of about 0.9 x 10^5 and 5.3 x 10^5 was noted, as shown in Figure 15. The separation point in this case was located at an angle θ of about 110°. This proves that Model C_2 has already entered the supercritical range at a wind velocity of about 10 m/s, which agrees well with the results of drag coefficient measurements.

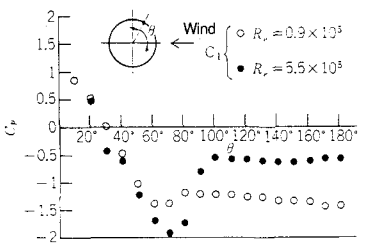

Figure 14 Pressure distribution over Model C_1

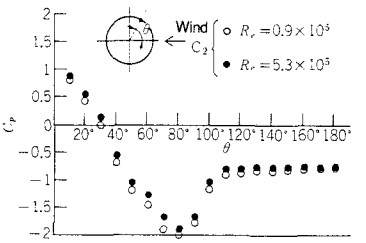

Figure 15 Pressure distribution over Model C_2

These results indicate that roughening the cable surface makes it possible to reproduce the supercritical state at wind velocities where rain vibrations occur. For models with smooth surfaces, no evident negative pressure peak is observed within the range of wind velocities at which rain vibrations occur. By contrast, with Model C_2, a negative pressure peak is observed at an angle θ of about 80° in the supercritical range. This negative pressure suppresses the formation of rivulets on the upper surface; such rivulets are one of the causes of rain vibrations. Pressure distribution measurements indicate that discrete roughness is estimated to suppress rain vibration by forming a negative peak pressure where water rivulets occur. The pressure distribution around inclined cable remains a problem for future research.

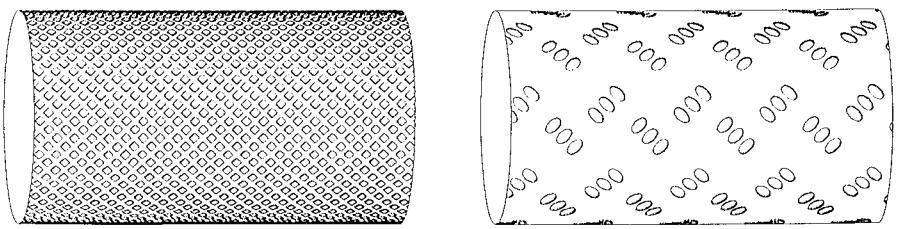

Model B_3 Model C_2

Figure 16 Cable surface appearance

5. ANALYSIS OF CABLE SURFACE PATTERNS

5.1 Analytical methods

In general, surface roughness is defined in terms of R_Z, the average peak-to-valley height, but this method fails to take the distribution of surface roughness into consideration. In this analysis, as a way to grasp not only the degree but also the distribution of surface roughness, the surface patterns of cable models were analyzed in greater detail. Since surface patterns can be regarded as irregular waveforms, they can be expressed mathematically as a Fourier series. The surface patterns of Models A, B, and C were modeled numerically as a) surface patterns in the form of sine waves, b) surface patterns with periodic rectangular waveforms, and c) surface patterns with waveforms consisting of a random step function. The arithmetic mean deviation of the roughness and the Fourier spectra were obtained for each. When expressing a surface waveform in terms of f(x), the average arithmetic mean deviation of the roughness R_a, is given by the following equation: $Ra = \frac{1}{\ell}\int_0^{\ell} |f(x)|dx$. Ra is calculated using evaluating length, ℓ, of 400 mm.

Table 3 Results of analysis of surface patterns

Model number	Relative surface roughness, k/D	Average arithmetic mean deviation of the roughness, R_a (mm)	Wavelength, L (mm)
A_6	1.2×10^{-2}	0.45	4.0
B_3	8.1×10^{-3}	0.41	11.1
C_2	1.1×10^{-2}	0.18	28.4

In spectral analysis, the intensity of a waveform is often defined by the energy spectrum, or $|x(f)|^2$. However, in this analysis of spatial surface waveforms, the Fourier spectrum x(f) was used. Figure 16 shows the appearance of cable Models B_3 and C_2, which were used in the analysis.

5.2 Results of analysis

Table 3 and Figure 17 show the results of analyzing typical surface patterns. By considering Ra, it was possible to gain an understanding of the average height of the surface roughness on each side of the line while taking the concave and convex patterns into account. Accordingly, where the surface roughness is uniformly distributed, the characteristics of the surface pattern can be expressed more precisely in terms of the average arithmetic mean deviation of the roughness than in terms of the apparent relative surface roughness, k/D.

As is clear from Figure 17, the Fourier spectrum is dominated by a certain wavelength, L, which means that, in the case of a non-uniform distribution of surface roughness, the surface pattern is a repetition of certain patterns at certain intervals corresponding to the dominant wave number (or inverse wavelength). That is, the amount of spread in surface roughness can be considered small when the repeated dominant wave number is small. Thus, the distribution of surface roughness can be found by calculating the dominant wave number.

We showed that the surface patterns adopted for cables used in this study had almost the same degree of relative surface roughness, but different average roughness height and surface roughness spread. Although this analytical method could not be correlated with the relationship between surface pattern and aerodynamic characteristics, the rough qualitative agreement with the measurements means that this analytical approach can be considered adequate. Further quantitative study of the relationship between the average surface roughness, distribution of surface roughness, and aerodynamic characteristics will be required, preferably using wind tunnel tests, numerical analysis, and so forth.

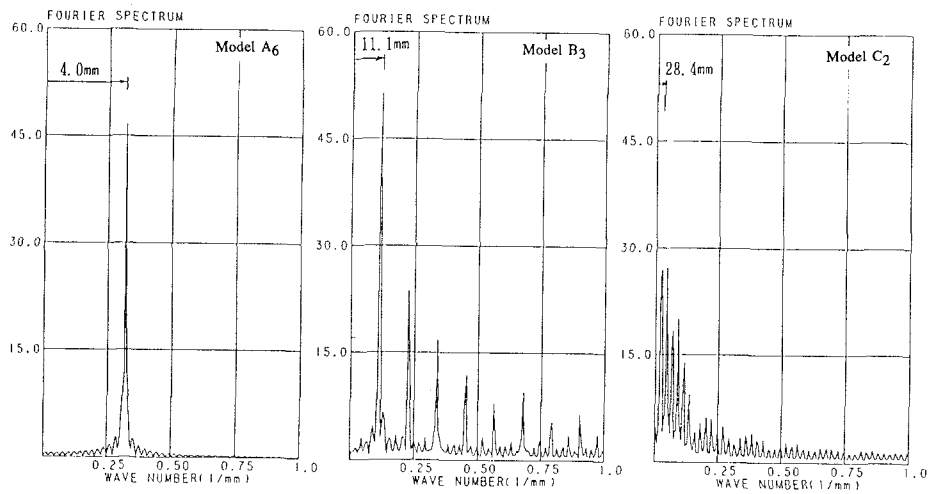

Figure 17 Fourier spectrum of cable surface patterns

6. CONCLUSIONS

In this study, the aerodynamic characteristics of cables with roughened surfaces and their rain vibration suppressing effects were studied experimentally in a wind tunnel test. For cables with a relative surface roughness of about 1% discretely of their diameter, the characteristics can be summarized as follows.

(1) The aerodynamic characteristics of cables with surface roughness vary considerably according to the shape and distribution of the roughness as well as the degree of surface roughness.

(2) The drag coefficient of cables with a discretely roughened surface is lower than that of cables with the same degree of uniform surface roughness. The drag coefficient of cables with a concave and convex pattern of roughness of about 1% of their diameter is about 0.6, which is just about the same as that of a smooth surface, for a Reynolds number of 5.5×10^5 (which is the design wind velocity region).

(3) Through rainfall experiments, it was ascertained that concave and convex patterns with a relative surface roughness of 1% of the diameter applied discretely on cable surface had rain vibration suppressing effects. Through the measurements of the location and width of water rivulets, those cables had effects of raising the apparent Reynolds number and making the flow separation point move backward.

(4) An analysis of the effects of surface roughness on the pressure distribution showed that the supercritical state equivalent to a wind velocity at which rain vibration occurred could be reproduced by adopting a pattern of concavities and convexities with a relative surface roughness of about 1% of the diameter. The suppression mechanism by which the formation of rivulets on the upper surface of model cables was also clarified.

(5) Differences between surface roughness, average surface roughness, and distribution characteristics were analyzed using model cables, with the aim of clarifying the factors influencing the differences. The quantitative relationship between surface roughness patterns and aerodynamic characteristics needs to be further studied.

(6) Before roughened surface cables are used in practice, further quantitative studies as regards design and manufacturing will be required.

The results of experiments on Models A and B are quoted partly from the "Study on Cable Vibration Tests" carried out by the Public Works Research Institute of the Ministry of Construction, The Civil Engineering Research Center, and Nippon Steel Corporation.[18] We wish to express our thanks to the research staff of Sumitomo Heavy Industries Co., Ltd. for their cooperation in the experiments and in the arrangement of experimental results for Model C.

REFERENCES

1) Higami, "Rain Vibration of Cables in Cable-stayed Bridges," Japan Association for Wind Engineering, Vol. 27, 1986

2) Yoshimura, Tanaka, Sasaki, Nakaya, and Hiki, "Rain-wind Induced Vibration of the Cables of the Aratsu Bridge," Proceedings of the Tenth Wind Engineering Symposium, 1989

3) Miyasaka, Nanso, Miyashita, Ushio, Nanjo, and Kado, "Measurements of Vibration in the Cables of the Ajigawa River Bridge," The 45th Report of the JSCE, 1990
4) National Land Development Technology Research Center, "Report on Study of Wind Resistance of Cables in Cable-stayed Bridges," 1989
5) Matsumoto, Shiraishi, Tsuji, and Hirai, "Research on Aerodynamic Vibration of Cables in Cable-stayed Bridges," Proceedings of JSCE, Vol. 416, 1990
6) Teramoto, Fujino, Ito, and Asaeda, "A Cross-sectional Analysis of Rivulets Occurring on the Upper Surface of Cables," Proceedings of Japan Association for Wind Engineering, Vol. 32, 1987
7) Yoneda, Maeda, and Iseki, "Damping Effects of Viscous Shearing Damper Newly Developed for Suppression of Vibration," Proceedings of the 11th Wind Engineering Symposium, 1990
8) Yokohama, Kusakabe, and Sekiya, "Study on Vibration Damping Effects of Interconnected Cables of Cable-stayed Bridges," Proceedings of the 12th Wind Engineering Symposium, 1992
9) Miyazaki, "Unstable Aerodynamic Vibrations and Prevention Methods for Cables in Cable-stayed Bridges," Proceedings of the 10th Wind Engineering Symposium, 1988
10) Matsumoto, Kitazawa, Ishizaki, Ogawa, Saito, and Shimodoi, "Wind-resistant Design of the Higashi-Kobe Bridge," Bridges and Foundations, 1991
11) Hojo, "Experimental Study on Rain Vibration Characteristics and Vibration Damping Effects of Cables of Cable-stayed Bridges," Proceedings of Japan Association for Wind Engineering, Vol. 50, 1992
12) Okajima and Nakamura, "Flow around Cylinder with Surface Roughness in the High Reynolds Number Range," Report of Applied Mechanics Laboratory, Kyushu University, 1973
13) Uematsu, Yamada, and Kikuchi, "Characteristics of Flow around Two-dimensional Cylinder with Surface Roughness," Proceedings of Japan Association for Wind Engineering, Vol. 43, 1990
14) Okauchi, Ito, and Miyata, "Wind-Resistant Structures," Maruzen, 1977
15) E. Simiu, "Wind Effects on Structures," John Wiley & Sons, 1986
16) Matsumoto, Shiraishi, Shirato, Hirai, Sano, and Katsura, "Study on Main Two Causes of Rain Vibration in Cable-stayed Bridges," Proceedings of the 11th Wind Engineering Symposium, 1990
17) Adachi, Matsuuchi, Matsuoka, and Kawai, "Flow and Resistance around Cylinders at High Reynolds Numbers," Proceedings of the Japan Society of Mechanical Engineers, Vol. 51, No. 461, 1985
18) Yokoyama, Kusakabe, Fujiwara, and Hojo, "Experimental Study on Cable Response to Vortex-induced Vibrations," Proceedings of the 12th Wind Engineering Symposium, 1992
19) Miyata, Yamada and Hojo, "Experimental Study on Aerodynamic Characteristics of Cables with Surface Roughness," Bridge and Foundation Engineering, Vol. 27, No. 9, 1993

(Received September 16, 1993)